In this chapter, we are presenting the preparation and characterization of "polyaniline/multiwalled carbon nanotubes/carboxymethyl cellulose" based novel composite material. It's morphological, thermal, structural and electrochemical properties were investigated by using different instrumental techniques. During the in-situ chemical polymerization of aniline in the aqueous suspension of CMC and MWCNTs, the particle size changes in two different ways "top to bottom" (low molecular weight oligomers grow in size) and "bottom to top" (long fibers of CMC fragmented in the reaction mixture). The combination of these two processes facilitated the fabrication of an integrated green-nano-composite material. In addition, a little amount of conductive nanofillers (MWCNTs) boosts the electrical and electrocatalytic properties of the material. Electron-rich centers of benzenoid rings exhibited π-π stacking with sp^2 carbon of MWCNTs. CMC dominantly affects the properties of PANI and negatively charged carboxylate group of CMC ionically bonded with protonated amine/imine. FTIR and Raman analyses confirmed that the material has dominating quinoid units and effective charge transfer. Hydroxyl and carboxyl groups and bonded water molecules of CMC result in the formation of a network of hydrogen bonds (which induces directional property). PANI/MWCNTs/CMC have nano-bead-like structures (confirmed from TEM analysis), large surface area, large pore volume, small pore diameter (BET and BJH studies) and good dispersion ability in an aqueous phase. Nanostructures of aligned PANI exhibited excellent electrochemical properties. Modified carbon paste electrode was used for electrocatalytic detection of ascorbic acid (as a model analyte). The sensor exhibited a linear range from 0.05 mM to 5mM, sensitivity 100.63 μA $mM^{-1}cm^{-2}$, and the limit of detection was 0.01 mM. We conclude from this study that PANI/MWCNTs/CMC

is suitable nanocomposite material to formulate electroactive ink and membrane for electrochemical sensor applications.

7.1 Introduction

Fabrication of multi-component advanced composite material is a straightforward way to compensate for the deficiencies of individual components. Such materials are complex in nature due to manifold interactions. Recent growth in the field of advanced instrumentation, new developments in material processing and fabrication of multi-component systems opens new directions for material research. Developing novel polymer-based nanocomposite material is an attractive area of research, particularly for sensor applications. Introducing natural polymer in a composite makes it environment-friendly. Green-nano-composite materials have following important characteristics: biodegradability, biocompatibility, nano dimension, large surface area etc. (Tiwari et al. 2009; Tiwari et al. 2012; Mantia et al. 2011; Mitra et al. 2014; Camargo et al. 2009).

Polyaniline (PANI) is the most studied intrinsically conducting polymer because it has interesting electrical, electrochemical and optical properties, easy synthesis, inexpensive monomer, environmental stability, nontoxic and variable oxidation states. Although there are certain limitations too, e.g. PANI could not be used as traditional thermosetting plastics, is insoluble in most of the solvents and it loses its conductivity in the neutral solution or at higher pH. For the desired application, the basic properties (solubility, redox properties, catalytic activity, and conductivity) of pristine PANI could be easily upgraded or tailored by using specific additives. During doping process, charge transfer takes place between polymer chain and anionic dopants, which perturbed the geometric parameters (bond length and

angles). The reversible conversions among various redox states and good conductivity of polyaniline make it an interesting electroactive electrode material (Zhao et al. 2011; Molapo et al. 2012; Dhand et al. 2011).

The synergy of nano and bulk material brings advances and novel properties in the composite system. A variety of nanoparticles have been used as nanofillers and templates for developing advanced nanocomposite materials. Reinforcing conducting nanofillers in the polymer matrix upgrade material properties and impart higher strength, large surface area, guided arrangement and better passage to the charge-diffusion (Dhand et al. 2011; Sabzi et al. 2010; Chen et al. 2010; Dhand et al. 2008).

CMC is inexpensive, nontoxic, biocompatible, environment-friendly, anionic semi-natural polymer. It is obtained from natural cellulose by chemical modification. CMC has chemically resistant, membrane forming and binding properties. Its interesting properties make this suitable for many technological applications e.g. toothpaste, laxatives, diet pills, water-based paints, detergents, textile sizing and conducting water-based ink. Hydroxyl groups and bonded water molecules of CMC make it soluble in hot and cold water and make it environmentally friendly. PANI/CMC based materials have been reported by many other research groups for a variety of applications, e.g. cholesterol biosensor, LPG gas sensor, supercapacitor and anti-corrosion coating (Yadav et al. 2011, Pasqui et al. 2014; Pahimanolis et al. 2013; Qiu et al. 2013; Barik et al. 2010; Ravikiran et al. 2014)

Vitamin-C, also known as ascorbic acid and L-ascorbic acid, is a naturally occurring organic compound. It is a mild reducing agent, antioxidant and an important metabolite in plants and animals. Vitamin-C is a water-soluble vitamin so it cannot be stored

in the body. It is necessary to get it from food, including citrus fruits, broccoli and tomatoes. Vitamin-C is required for the growth and repair of tissues making skin, cartilage, tendons, ligaments, blood vessels etc. Ascorbic acid and its sodium and potassium salts are commonly used as antioxidants and preservatives in food industries. It is oxidized with a loss of one electron to form a radical cation and then with the loss of a second electron to form dehydroascorbic acid. It typically reacts with oxidants of the reactive oxygen species, such as the hydroxyl radical. On exposure to oxygen, ascorbic acid will undergoes oxidative decomposition to various products. Determination of ascorbic acid is very important in many areas e.g. electrochemistry, neurochemistry, pharmaceutical preparations, foodstuffs and clinical diagnostics (Ravikiran et al. 2014; Rivero et al. 2012; Chairam et al. 2011; Roya et al. 2011; Tiwari et al. 2012). In this work, we have used Ascorbic acid (vitamin-C) as a model substance to investigate the electro catalytic property of the developed nanocomposite material.

Polyaniline/polysaccharides composite systems are an interesting area of research due to their low cost, stable redox properties and interesting nano-morphologies. Distinct properties of PANI/Polysaccharides composite systems motivated us to comparatively investigate a series of such materials. We have studied the important characteristics of PANI/MWCNTs/Starch composite material earlier. Starch consists of two types of molecules: the linear and helical amylase (soluble) and the branched amylopectin (insoluble). Amylose is a much smaller molecule than amylopectin. CMC and starch interactions with polyaniline are significantly different (Gautam et al. 2017; Gautam et al. 2016). On one hand, starch has micro size granular morphology, while CMC is fibrous. Starch granules do not swell in cold water, however, in hot water they absorb water and rupture, whereas CMC

is more soluble and gives a viscous solution in normal water (10 mg/ml). The carboxyl group of CMC gets ionized at higher pH and it could interact with polyaniline more effectively than starch. In addition, CMC is a proven material for membrane and conducting inks formulation. Conductivity and electro-activity are the required quality of an electrode material (especially for electroanalytical applications).

These facts motivated us to investigate the important characteristics of PANI/MWCNTs/ CMC composite. We have studied the impact of CMC and MWCNTs on the major properties of Polyaniline. Efforts are going on to fabricate paper strip biosensors.

7.2 Experimental Section:

7.2.1 Materials:

Aniline (C_6H_7N) (99%) was purchased from Merck, ammonium peroxydisulphate (APS) [$(NH_4)_2S_2O_8$], Hydrochloric acid and acetone were used as received from Qualigens Fine Chemicals India, Carboxymethyl cellulose (CMC) was purchased from Loba Chemie (AR grade), Ascorbic Acid was purchased from Sigma Aldrich. MWCNTs prepared via chemical vapor deposition technique [NANOCTC 7000, FRAHN, HOFFER IPA, July 2013, MRTIRMATIS]. Double distilled water was used for the preparation of all solutions.

7.2.2 Instrumental Characterization:

FTIR spectra were recorded by using Perkin Elmer Spectrum version 10.03.05 with a range of 4000-500 cm^{-1} with potassium bromide (KBr) pellets at room temperature. The Raman spectra were collected by using a Renishaw Raman spectrophotometer equipped

with a microscope Model: MX50 A/T Olympus. Electronic spectra were measured by using Varian Carry 100 Bio dual beam spectrophotometer, in the wavelength region 200 to 900 nm, scan rate of 400nm/min (sample preparation-paste of 0.05g sample and 4g $BaSO_4$). The crystalline properties of materials were investigated by Ultima IV X-ray diffractometer with Cu-Kα radiation (λ = 1.5404 Å), with a scan speed of 10° min^{-1}. Scanning electron microscope (SEM) images were taken by using Quanta 200 Company- FEI of USA (SEA) PTE Ltd., Singapore at suitable voltages and magnifications. Transmission electron microscopy (TEM) examination was made by using FEI Company Technai 20G2 electron microscope at an accelerating voltage of 200 KV. Atomic force microscopy (AFM) characterization was performed with the DI Nanoscope IIIa microscope of the LNLS in non-contact mode, NSC-10-50, » 20N/m at » 260 KHz. Surface area analysis by using nitrogen adsorption/ desorption isotherms measured by Micromeritics ASAP-2020 physisorption instrument. Thermal analysis (TGA and DTA) was carried out by NETZSCH STA 449 F3 Jupiter in the temperature range 0°C to 300°C. Electrochemical experiments were carried out with model 600-D Series electrochemical analyzer, CH instruments, USA.

7.2.3 Preparation of Composite Material

Four materials (PANI, PANI/MWCNTs, PANI/CMC and PANI/ MWCNTs/ CMC designated as system 1, 2, 3 and 4 respectively) were prepared by chemical polymerization of aniline in 0.1 M HCl using ammonium peroxidisulfate as oxidizing agent. Initially, 0.2 mg MWCNTs was ultra-sonicated in 4 ml aniline for 30 minutes. The ratio of aniline to the oxidizing agent was 1:1.25, for achieving the best yield. Dilute solution of the

oxidizing agent was added dropwise in the homogeneous suspension of 0.5 M aniline, 0.1 M HCl, CMC and MWCNTs. The ratio of aniline: CMC was 1:1 w/w in the reaction mixture. It was continuously stirred for 2 hours and kept for 24 hours undisturbed to complete polymerization. The reaction yielded a dark green colloidal product that was washed three times with 0.1 M HCl and Acetone, and dried in hot air oven (60°C for 24 hours).

7.2.4 Fabrication of Carbon Paste Electrode:

Carbon paste electrode was fabricated by using glass capillary as electrode body (2 mm diameter) and clean copper wire for connection. Carbon paste was prepared by 10 mg sample, 90 mg fine quality graphite powder and 10 µl Nujol oil, using a mortar-pestle for manual mixing. Out of this, 2 mg paste was filled in the capillary and the surface was smoothened using a clean butter paper.

7.3 Results and Discussion:

7.3.1 Mechanistic Aspects: Composite Material Formation:

The composite was prepared by in-situ free radical chemical polymerization of Aniline in the aqueous suspension of CMC and MWCNTs (molecular structure and photograph of individual components are given as *c.f. C1*). The mechanism of in-situ chemical polymerization of aniline is well reported in the literature. Polyaniline formation via free radical polymerization consists of following important steps viz. oxidation of the monomer, radical coupling and rearomatization, chain propagation, oxidation, doping, chain termination and reduction of pernigraniline salt to emeraldine salt (Gautam et al. 2016; Sapurina et al.

2008; Tiwari et al. 2012). In this work, we have used aniline within the aqueous suspension of CMC and MWCNTs acidic solution and the process followed the same mechanism as reported earlier, however, the presence of additives certainly has an impact on the arrangement of polymer chains. During the process of composite formation, size of particles changed in dual direction: bottom to top (low molecular weight oligomers grow in size as long polyaniline chain) and top to bottom (CMC fibers degraded into smaller fragments). In acidic medium, Aniline monomer gives radical cation (anilinium ion), which coupled with another monomer to form dimer. On successive chain propagation oligomers and polymers were formed. SEM image confirmed the fragmentation of CMC fibers *(c.f. C1B)*. Thus, we could say that simultaneously various phenomena were taking place that can be listed as: degradation and oxidation of polysaccharide, polymerization of aniline and the formation of Polyaniline-Polysaccharide composite. In addition, aromatic structures of PANI interacted with the basal plane of MWCNTs through π-π stacking. The sp2 carbons of the MWCNTs could compensate the positive charge on Polyaniline chains. CMC improves MWCNTs dispersion in an aqueous medium and could interact with PANI (Tiwari et al. 2012; Zhao et al. 2012). CMC has a balance of hydrophilic (-OH, C-O-C) and hydrophobic (-CH, -CH_2-) region. The glucose rings are connected with β-1, 4 glycosidic linkages. The carboxy methyl groups exhibited pH dependent anionic character, in free acid form (neutral) at pH 3.5, and ionized acid form (negatively charged) at about pH 7.0. The bulky anionic groups could make ionic bonds with protonated PANI and such interactions suppressed deprotonation. Washing with 0.1 M HCl and Acetone not only removes residual monomers/oxidant/ decomposition products/oligomers but also produces uniformly

protonated composite. The dark green color of composite indicated that the polyaniline was in emeraldine salt form.

7.3.2 Morphological Studies:

7.3.2.1 SEM and TEM Analysis:

Electron microscopic images reveal the micro/nanostructural information about the materials. Figure 7.1 shows the scanning electron microscopic images of PANI, PANI/ MWCNTs, CMC, PANI/CMC and PANI/ MWCNTs/CMC. Non-uniform granular aggregation was observed for pristine PANI due to multilevel irregular secondary growth (fig. 7.1A). MWCNTs are conducting nanofiller and act as nano template, which result in a guided deposition of PANI, so PANI/MWCNTs exhibited a core-shell structure (fig.7.1B). CMC has smooth cylindrical micro-fibrous structure, diameter ~ 20 μm (fig.7.1C, D). We have treated CMC and Starch with the acidic solution of ammonium peroxydisulphate (oxidizing agent) and investigated the resulting structural change (Gautam et al. 2016). Starch is partially soluble in the reaction mixture, so no significant change is observed in the shape and size of the granules, whereas long CMC fibers were fragmented into small particles *(c.f. C1B).* The solubility of CMC is affected by many parameters like nature of solvent, viscosity, the degree of substitution and shear rate. During the composite formation, CMC tends to aggregate and form lumps rather than an instant solution. These small fragments slowly dispersed in the reaction mixture, followed by the formation of colloidal solution and/or CMC hydrogel (no particle is visualized in low concentration aqueous solution of CMC *(c.f. C6A).* CMC fragments act as substrate for PANI deposition and hence fragments seem to be scattered in the matrix. PANI/CMC has non-uniform

morphology (fig. 7.1 E, F). Molecular conformations and rearrangement of polymers within a composite are greatly influenced by the extent of inter/intra hydrogen bonding and the presence of template/nanofillers. Hydroxyl and carboxylic groups of CMC promote multiple inter/intra hydrogen-bonds of the constituents of composite material, whereas SP^2 carbon of MWCNTs brings pi–pi-stacking of polyaniline chains. Strong interfacial interactions facilitated the uniform dispersion of MWCNTs. The hydrogen bond network and nanofillers increase the strength and density of the material (sharp signal in the Raman spectra confirm the compactness of nanoparticles). PANI/MWCNTs/CMC has compact, uniform and integrated morphology (fig. 7.1G, H). TEM is an appropriate technique to observe the shape and size of particles at nanoscale resolution. Impact of nanofillers on the morphology of composite material is also observed. The system-3 has an irregular shape and non-uniform thickness (fig. 7.2 A, B, C), whereas system-4 has linearly aligned compact bead-like structure (diameter ~ 50 nm), because hydrogen bonds and pi-pi stacking bring guided deposition of particulates (fig. 7.2 D, E and F).

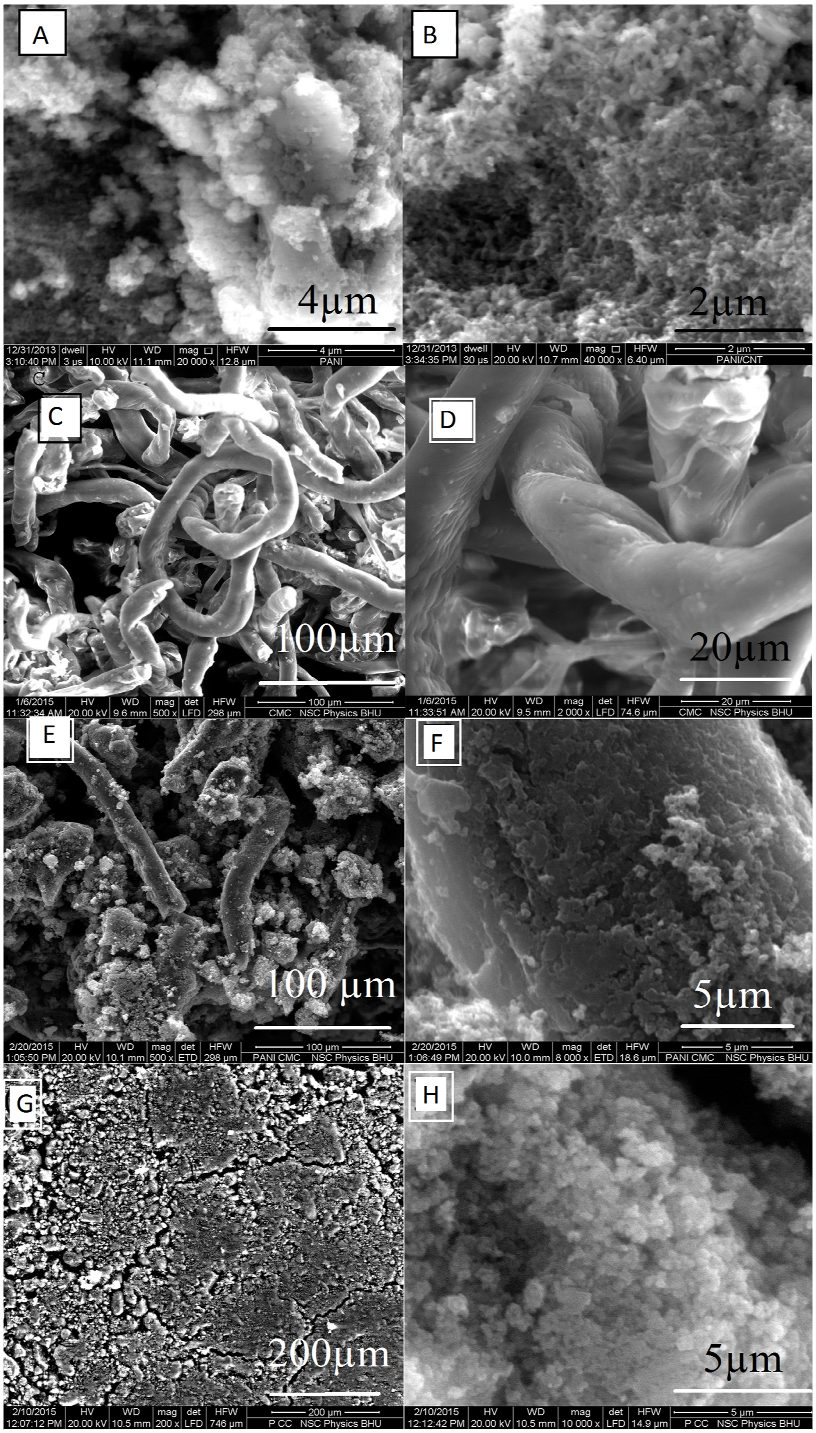

Fig. 7.1 SEM micrographs at different magnifications (A) PANI (B) PANI/MWCNTs (C-D) CMC (E-F) PANI/CMC (G-H) PANI/MWCNTs/CMC

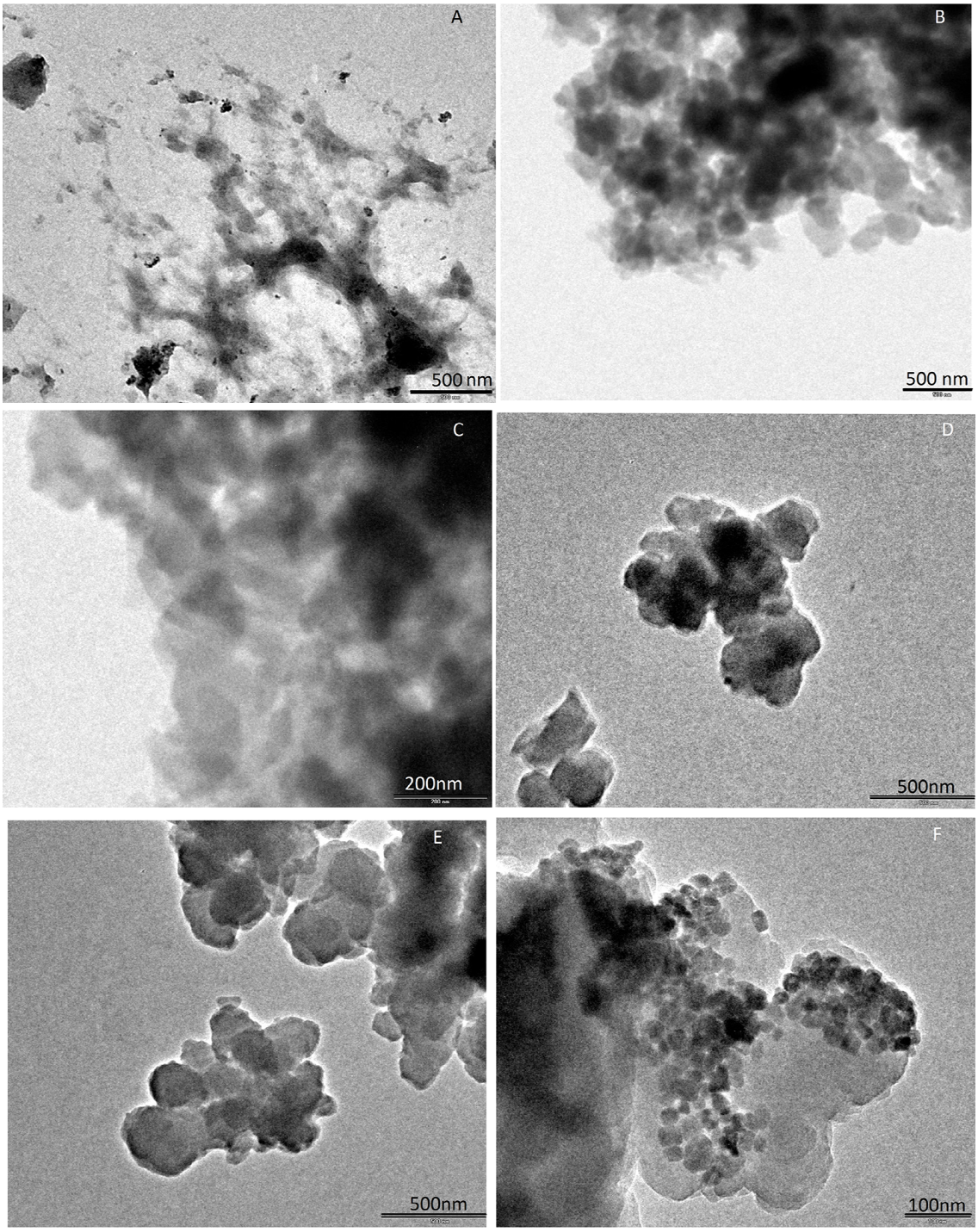

Fig. 7.2 TEM micrograph of system-3: PANI/CMC (A, B and C) and system-4: PANI/MWCNTs/CMC (D, E and F)

7.3.3 BET Surface Area Analysis:

Catalytic and adsorption properties of the material depend on surface area and porosity. Nitrogen adsorption/desorption isotherms were measured at 77 K for surface area and pore-size distribution. Effect of additives on the BET surface area and BJH pore width of pristine PANI was measured by comparing system 2, 3 and 4 with system-1 (data for BET and BJH analysis is given as *c.f. C2A, B*). We observe that system-4 has largest average surface area and cumulative pore volume, however, it has a smaller pore diameter. So, we can say that system 4 has nano-porous architecture, as a result higher redox peak current and better electro-catalytic activity (confirmed from CV analysis). We inferred that: (a) addition of MWCNTs, increases surface area 6389%, pore volume 261%, and decreased the pore width 4% (on comparing system 2 and 1) (b) addition of CMC, increased the surface area 3296%, pore volume 94 %, and decreases pore width up to 2.74 % (on comparing system 3 and 1) (c) with the addition of MWCNTs and CMC, in synergy the surface area increase by 46501%, pore volume 678 %, but the pore size decreased by 1.5 % (on comparing system 4 and 1).

7.3.4 Spectroscopic Analysis:

7.3.4.1 FTIR Spectroscopic Analysis:

The FTIR spectra of materials were measured to investigate structural information, the spectral range of 4000-400 cm^{-1} (fig. 7.3). Important vibrational frequencies obtained for the different systems have been tabulated for easy comparative studies *(c.f. C3)*. The shift in NH stretching frequencies 3000-3300 cm^{-1} and 1139 cm^{-1} (on comparing system-1 and 2) is attributed to π-π stacking between PANI and MWCNTs. The electrostatic interactions and

charge transfer reactions perturbed hydrogen bonding (Gautam et al. 2017; Gautam et al. 2016). Proton donor-acceptor system and effective orbital overlapping, lead to inter and intramolecular hydrogen bonding, which could be considered as an important factor responsible for particle orientations. The extent of hydrogen bonding was revealed from the significant variation in stretching frequencies at 3454 cm^{-1} attributed to hydroxyl groups. The relative increases in peak intensity confirm the presence of more quinoid units than benzenoid units (at stretching frequencies at 1580 cm^{-1} and 1462 cm^{-1}). The disappearance of peaks at 1293 cm^{-1} and 1234 cm^{-1} is attributed to perturbation of the conjugated system. CMC exists as protonated form at low pH, attributed to a sharp peak observed at 1738 cm^{-1} for carboxylic acid (Li et al. 2013; Rao et al. 2000; Chiem et al. 2008). Thus, during the formation of composite preparation, the negatively charged carboxylate group of CMC has ionic interactions with the protonated amine of polyaniline (for system 3 and 4). It is confirmed that the developed composite system is a multi-functional material. 3462 cm^{-1} (-NH-), 3212 cm^{-1} (-OH), 2918 cm^{-1} (-CH), 1734 cm^{-1} (Amide linkage or COOH group), 1609 cm^{-1} (C=C stretching), 1556 cm^{-1} (quinoid unit), 1484 cm^{-1} (benzenoid unit), 1600 cm^{-1} , 1475 cm^{-1} and 1403 cm^{-1} (C=C stretching in aromatic compounds often occurs in pairs), 1300 cm^{-1} (C-O ether linkage), 1230 cm^{-1}, 1139 cm^{-1} (N=Q=N). C-Cl stretching (590-700 cm^{-1}) shows shifting of peaks and confirms the perturbation of Chloride-PANI interactions; this confirms that CMC and MWCNTs are also competent dopants, and they could replace chloride ions. The developed material has extensive hydrogen bonding due to the presence of numerous hydroxyl groups and bonded water molecules (confirmed from the broad and strong peak for -OH stretching at 3462 cm^{-1}). The amide linkage between PANI and CMC

was confirmed from peaks at 1734 cm^{-1} and 1609 cm^{-1}. The biocompatibility of the material has been predicted on the basis numerous amino and hydroxyl groups.

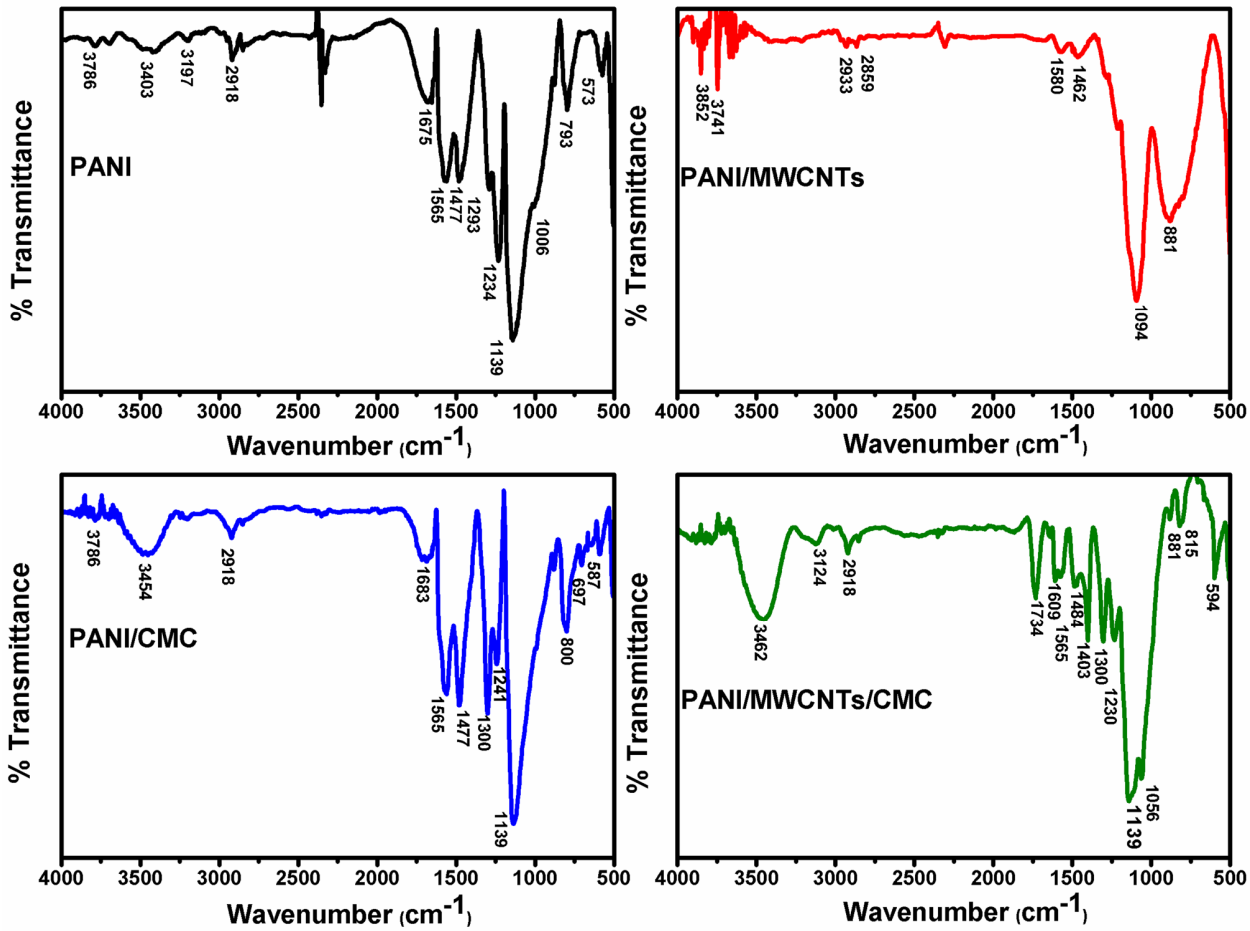

Fig.7.3 FTIR spectrum (A) PANI (B) PANI/MWCNTs (C) PANI/CMC (D) PANI/MWCNTs/CMC

7.3.4.2 Raman Analysis:

Raman spectroscopy is highly sensitive to the morphology and electronic structures of material. Raman conditions are not the same for distinct oxidation states and protonation levels of PANI. System 1, 2, 3 and 4 showed significantly different spectra, measured in the frequencies range from 400-1800 cm^{-1} (fig. 7.4). The characteristic peaks for PANI at 1617 cm^{-1} (stretching mode in the phenyl rings), 1500 cm^{-1} (stretching C=N and C=C in quinone),

1327 cm^{-1} (stretching vibration of C-N^{+}), 1230 cm^{-1} (C-C benzenoid ring deformation), 1190 cm^{-1} (C-H bending vibration of semiquinone rings), 827 cm^{-1} (benzene ring deformations), 590 cm^{-1}, 512 cm^{-1} (out-of-plane deformations of the ring). "Raman effect" leads to sharp and strong peaks due to the frequency of incident radiation coinciding with the frequency of electronic transition (Nascimento et al. 2008; Silva et al. 2005; Arsov et al. 1998).

System-2 has sharp and intense peak than system-1 because compact particles exhibit greater scattering. Presence of MWCNTs guided the arrangement of PANI chains in an efficient way and this interaction leads to the formation of more quinoid units and bipolarons, (confirmed from the shifting of peak at 1614 cm^{-1} towards lower frequencies, sharp & intense peak at 1478 cm^{-1} and 1100-1140 cm^{-1} region attributed to better charge delocalization and weak peak 1329 cm^{-1} and 1220 cm^{-1} attributed to C-H bending of benzenoid ring). MWCNTs facilitate the charge delocalization along the chain and also inter-granular charge transfer, confirmed from the peak shift toward the lower frequency (1190 cm^{-1} for system-1 and 1158 cm^{-1} system-2).

On comparing system-3 and 4, we infer that small amount of nanofillers significantly perturbed the chain arrangement and morphology of PANI/CMC. Important peaks observed in the spectra for system 3 and 4 are 1530 cm^{-1}, 1491 cm^{-1}, 1350 cm^{-1}, 1287 cm^{-1}, 1224 cm^{-1}, 1073 cm^{-1}, 742 cm^{-1}, and 536 cm^{-1}; 1700 cm^{-1}, 1600 cm^{-1}, 1510 cm^{-1}, 1434 cm^{-1}, 1280 cm^{-1}, 949 cm^{-1}, 741 cm^{-1}, 610 cm^{-1}. The appearance of a peak at 1700-1600 indicates polymer chains are linearly arranged along the nanotube's walls, associated with stretching mode of the phenyl ring and higher polaron formation. Other than that, 1500-1400 cm^{-1} (associated with in-plane deformation of the C-C bond of the quinoid ring) and a sharp peak at 741 cm^{-1} (associated with deformation vibrations of the aromatic rings) are also observed. There are

higher intensity bands at 1324-1375 cm^{-1} (associated with C-N, C=N, polarons delocalization) and 1450 -1500 cm^{1} (associated with C-N modes in quinoid units).

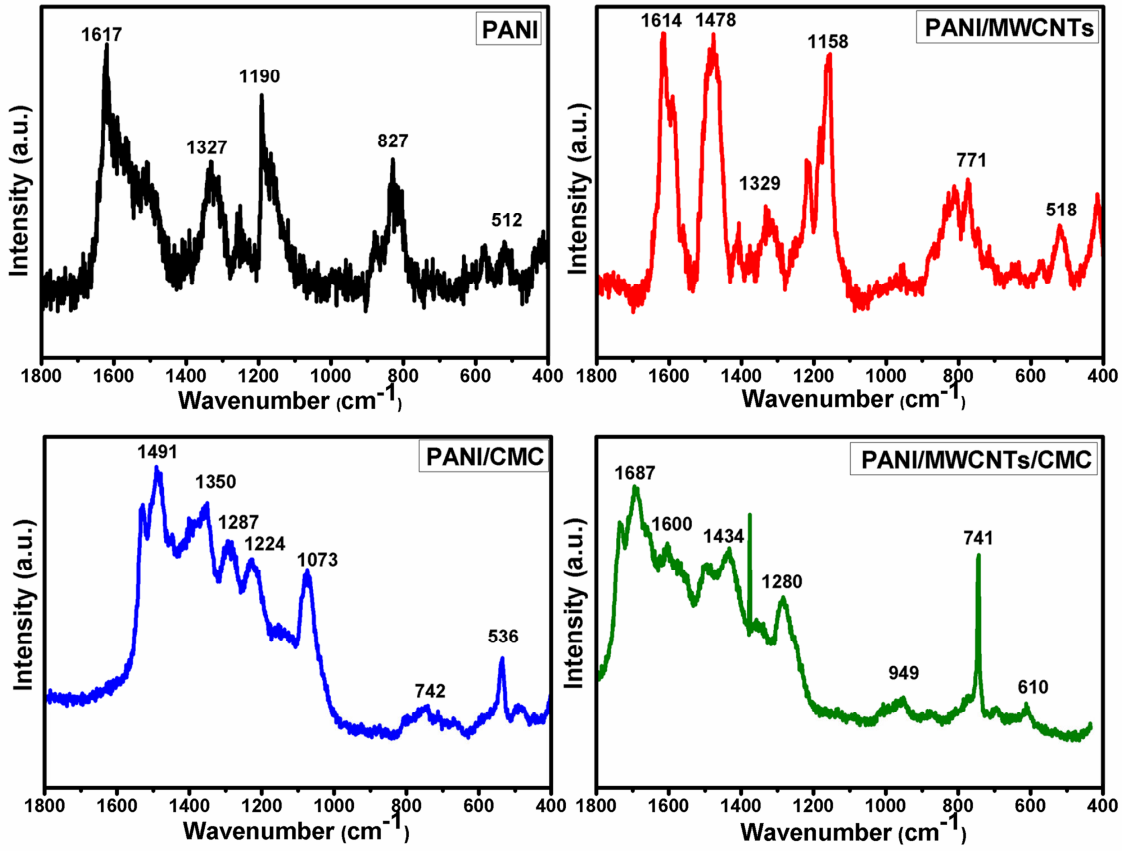

Fig. 7.4 Raman spectrum (A) PANI (B) PANI/MWCNTs (C) PANI/CMC (D) PANI/MWCNTs/CMC

7.3.5 UV-Vis Spectroscopy:

Electronic spectroscopic analysis of PANI based materials showed following absorption bands: ~ 320 nm (π-π* transition in the benzenoid ring), ~ 418 nm (protonation of PANI; polaron and bipolarons), ~ 610-650 nm (exciton formation and π-π* transition of quinoid rings) and ~ 800nm (protonation of imine site) (Gautam et al. 2017; Gautam et al. 2016; Ali et al. 2012; Abdiryim et al. 2012). The peak intensity ratio of π-π* to n-π* transition indicates the relative number of oxidized and reduced units in

the PANI chain. The higher intensity in the region at 800 nm suggests the effect of doping in the composites. System-4 has higher absorption in the region 310-320 nm and 400-450 nm (π-π* transition in the benzenoid ring and protonation of PANI, polaron, and bipolarons) and thus confirms good conductivity and greater charge delocalization *(c.f. C3B).* Doping of MWCNTs, CMC and Chloride ions effectively compensated positive charge of PANI. The value of E_g for the direct transition was obtained from extrapolation of the straight line portion of $(\alpha h\nu)^2$ versus $(h\nu)$ on the $h\nu$ axes (Data not shown here). Incorporation of $MWCNT_S$ reduces the bandgap energy, attributed to intermediate conduction bands between the energy bands of pristine PANI (4.9 eV to 4.85 eV). Incorporation of CMC insulates the inter-chain charge transfer (bandgap increased from 4.9 eV to 4.95 eV). Interchain insulation overcome by using MWCNTs in PANI/CMC (band gap reduces from 4.95 eV to 4.92 eV).

7.3.6 X-ray Diffraction:

Polymer chain arrangements, internal stress and lattice parameters could be investigated by using X-ray powder diffraction. The X-ray diffractograms of pristine PANI, PANI/MWCNTs, PANI/CMC and PANI/MWCNTs/CMC show that the pristine PANI powder exhibits three broad peaks (2θ ~14.87°, ~20.99° and ~25.15° - corresponding to 011, 020 and 200 planes of benzene rings in adjacent chains), which is attributed to partial crystalline nature (*c.f. C4A, B*) (Gautam et al. 2017). However, additives lead the distorted chain arrangement, i.e. the d spacing increases with the addition of MWCNTs. The Scherrer equation ($D = 0.9\ \lambda\ /\beta\ \text{Cos}\ \theta$) was used to calculate the crystal size D (nm) of the studied samples, where λ is the wavelength of the X-ray source (Cu Ka

=1.518 Å) and β is the full width at half maximum (FWHM) of the X-ray diffraction peak at the diffraction angle θ. The Scherrer equation was used to calculate the crystallite size. Peak width is inversely proportional to crystallite size and hardness. PANI has a limited chain arrangement during traditional chemical polymerization and show globular morphology as confirmed by SEM and TEM analysis. So, we have observed a small crystallite size for pristine PANI. However, with MWCNTs the crystallite size increases from ~ 4.42 nm (for system-1) to ~6.88 nm (system-2), which is attributed to the long-range ordered arrangement of PANI chains at nanotubes surface. Small crystallites were combined together as a bigger particle. The data support the fact that MWCNTs act as template/nanofillers, which leads to an ordered arrangement. Higher intensities of the peaks indicate an improvement in inter-chain π-π stacking and elongation of the effective conjugation length (which result from a facilitated charge transport). Small fragments interact with PANI chains, as a result, we observed comparatively bigger crystallite size ~ 6.46 nm (system-3) and ~ 6.47 nm (system-4). System-4 has compact nano size granular structure.

7.3.7 Thermal Analysis:

Thermal stability of the material was investigated by using thermal techniques. TGA and DTA experiments were carried out in the nitrogen atmosphere with heating rate: 10°C/min and heating range: room temperature to 300°C. Three important events are responsible for weight loss in PANI based material in the temperature range from 80 to 140°C: desorption of water and encapsulated moisture, from 140 to 200°C: expulsion of dopant/hydroxyl groups/bonded water molecules and from 200 to 450°C: thermal degradation of the PANI structure and loss of small molecules/fragments (Wei et al. 2003). The

composite materials exhibited higher decomposition temperatures than pristine PANI. Materials show differences in weight loss in the different temperature range. Weight loss starts at temperature 70°C, 100°C, 80°C and 110°C for system-1, 2, 3 and 4, respectively. System-3 and 4 show a higher weight loss about 35%, attributed to numerous hydroxyl group of CMC and bonded water molecules. MWCNTs improve the stability of materials at ambient temperature (system-2 and system-4), CMC based composite material (system-3 and system-4) shows larger weight loss (~35%) at a temperature higher than 200°C (attributed to a large number of hydroxyl groups). System-2 is most stable due to its compact morphology and hydrophobic nature of MWCNTs, whereas system-3 is less stable (attributed to weak hydrogen bonding and hydroxyl groups). In synergy, MWCNTs and CMC improve the stability of the system-4 up to 200°C, attributed to integrated compact morphology and better binding ability (confirmed from other analysis). At 300°C, The residual weight obtained for different systems are: 75% (1), 80% (2), 65% (3), 64% (4) (fig. 7.5). In DTA analysis, temperature changes were recorded relative to an inert reference while both undergo similar thermal cycles. This differential temperature is plotted against time (DTA curve), or against temperature (thermograms). DTA curves are useful to investigate exothermic or endothermic process relative to the inert reference, type of transformations (glass transitions, crystallization, melting and sublimation) and used as a fingerprint to identify a specific material. It is very important to notice that incorporation of MWCNTs improved the thermal stability of material and heat capacity of the systems. We inferred that system-4 adsorbed more heat than other systems at 300°C, attributed to compactly integrated morphology and strongly bonded dopants with PANI chains.

Temperature Range (°C)	System-1 % Wt. loss	System-2 % Wt. loss	System-3 % Wt. loss	System-4 %Wt. loss
50-100	2	0	1	0
100-150	5	3	12	3
150-200	14	7	14	10
200-300	25	20	35	35

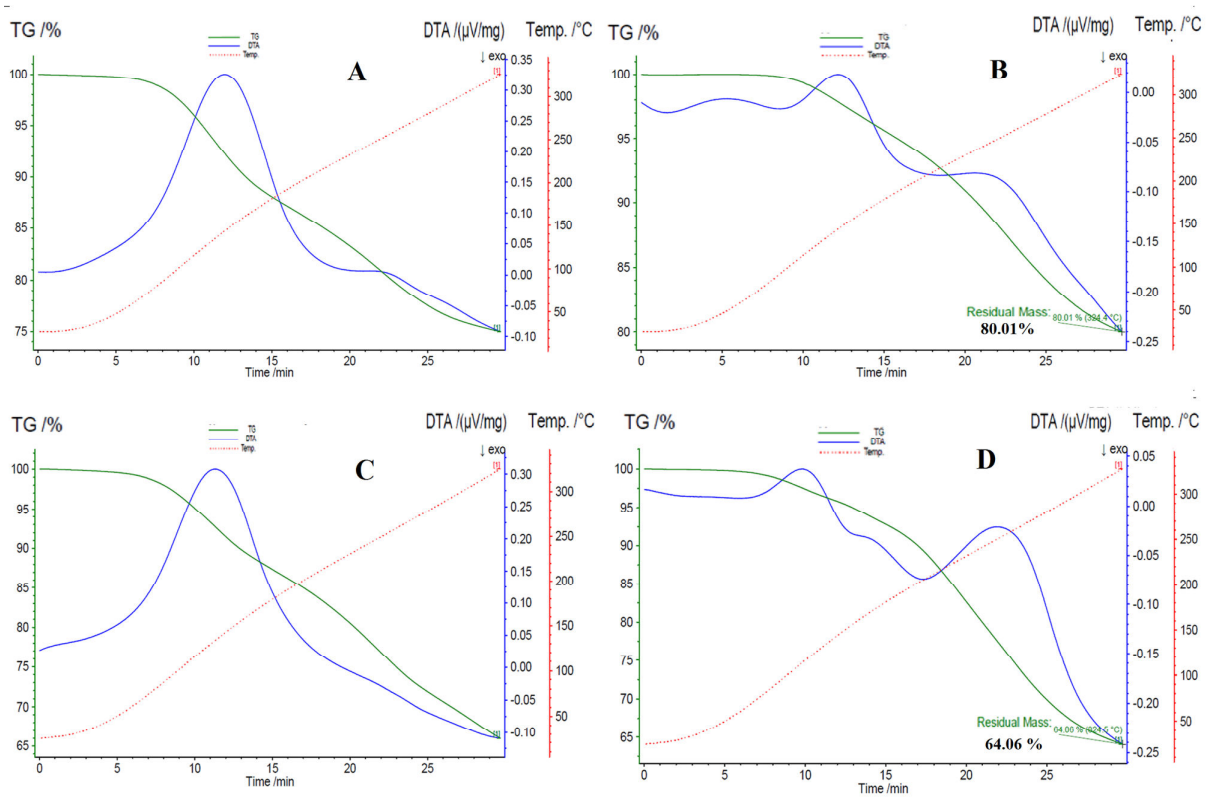

Fig. 7.5 TGA and DTA analysis at a heating rate of 10 °C min^{-1} in nitrogen; (A) PANI,(B) PANI/MWCNTs, (C) PANI/CMC, (D) PANI/MWCNTs/CMC

7.3.8 Electrochemical Studies:

7.3.8.1 Cyclic Voltammetry:

CV is an excellent technique to study electrochemical properties of materials and other electrode processes. During CV analysis the current response is measured with respect to applied cyclic potential (E). It associates with following phenomena: capacitive currents (double layer charging), faradic current (oxidation/reduction of electroactive species/ions) and adsorption/desorption (Kissinger et al. 1983). The electrochemical behavior of PANI has been well studied by many researchers (Dhand et al. 2011; Tiwari et al. 2012; Gautam et al. 2017). Among the three constituents of the composite, only PANI has electroactivity that has significantly improved by using additives. Carbon paste electrodes are low cost, renewable and easy to fabricate. Carbon paste electrode has been fabricated in various ways and found application in many technological areas (Svancara et al. 2009; Vytras et al. 2009).

One of the major objectives of this research work is to develop a low- cost sensor. Carbon ink has been proven a commercial material used for screen-printed electrode. The cyclic voltammograms were measured by using a conventional three-electrode system (PANI/MWCNTs/CMC modified carbon paste, Pt wire and Ag/AgCl-saturated with KCl were used as working, auxiliary and a reference electrode, respectively. The phosphate buffer solution (0.1 M at pH 7.0) was used as supporting electrolyte solution. We herein used a glass capillary, diameter 2 mm, as an electrode body and copper wire used for the electrical connection *(c.f. C 5A)*. Effect of scan rate on the CV was measured by running an experiment in 0.1M HCl (in order to nullify the deprotonation process) at scan rates 200, 100, 50, 10 mVs^{-1}in a potential range -400 to +800 MV (fig. 7.6). Peak current increases at higher scan rate attributed to higher diffusion. MWCNTs displayed a great impact on the electron exchange process

and better electro-activity, attributed to a large surface area and greater bulk conductivity of the material. System-4 is better in terms of better charge transfer at lower threshold potential than others.

Effects of pH on the CV was measured by using different PBS solutions having pH- 1, 3, 5 and 7 *(c.f. C5B)*. A local ionic concentration of material is indeed a function of pH. At lower pH, two redox couples are observed, indicating that two different redox processes were taking place i.e. proton (lower potential) and anion (higher potential) doping/dedoping, respectively. At higher pH, lower proton concentration in the test solution, leads to poor proton exchange- the associated redox couple diminished and a single redox couple was observed. In more acidic solution, an increase of ion diffusion coefficient and the protonated chain has extended charge delocalization and low electrical resistivity. The reduction peak shifted toward more negative potential than oxidation peak. Large peak separation and low peak current are associated with sluggish electrode kinetics and deprotonation.

Ascorbic acid is an electroactive compound, gets oxidized at 700 mV on a bare platinum electrode, but it may foul the electrode surface due to oxidative products. Other than that, oxidation at higher positive voltage potentially increases the risk of interference (present in sample matrix). To overcome this problem, electrode surface has been modified with suitable electroactive materials. It increases the selectivity and charge transfer capability at the electrode surface. Application of the developed advance green-nano-composite materials as electrode material exhibited many advantages such as better electrocatalytic properties, higher surface area, selectivity and desired functionality. The CV response of 1 mM ascorbic acid was measured on

modified carbon paste electrode (for system-3 and 4) at scan rate 5 mV/s potential range -200 and +600 mV, step potential +6 mV and (fig. 7.7). Ascorbic acid was electro-catalytically oxidized at the lower potential on modified carbon paste electrodes than bare electrode (system-4 ~350 mV and system-3 ~500 mV). The higher anodic peak current indicates better sensitivity (system-4 = 95 µA, system-3=77 µA) attributed to nano effects of MWCNTs i.e, fast electrode kinetics, higher conductivity and large surface area. The response of some other analytes was also measured; the greater current response for ascorbic acid indicates that the developed material is more sensitive to Ascorbic acid than others *(c.f. C5C)*.

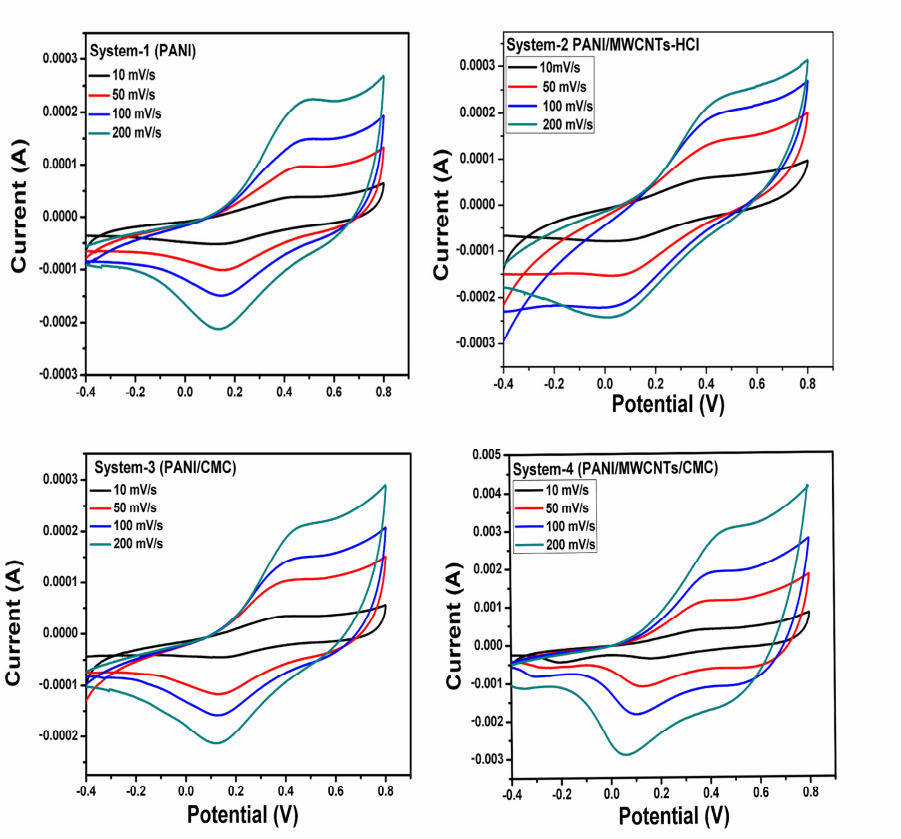

Fig. 7.6 Cyclic voltammograms for system-1-4 at different scan rate in 0.1 M HCl.

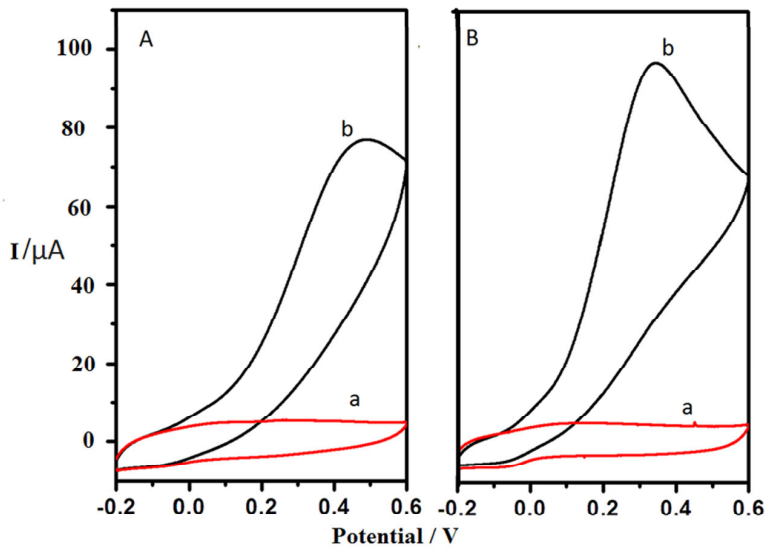

Fig. 7.7 Cyclic voltammograms for system-3 (A) system-4 (B) in 0.1 M PBS-7 at 5 mV/s; Curve "a": Blank, Curve "b": 1 mM Ascorbic acid

7.3.8.2 Amperometric Studies:

The amperometric measurement of ascorbic acid (for system-3 and system-4) was carried out at 100 mV under stirred conditions. 95 % of the steady-state current was attained within a reaction time 5 s (fig. 7.8 A). The composite electrode exhibited a linear response to ascorbic acid. The linear range of the detected ascorbic acid was 0.05 mM to 5mM with a correlation coefficient of 0.9860, sensitivity 100.63 μA $mM^{-1}cm^{-2}$ and limit of detection 0.01 mM (S/N=3) (fig. 7.8 B). Thus, we could easily conclude that system-4 is a better electrode material than system-3.

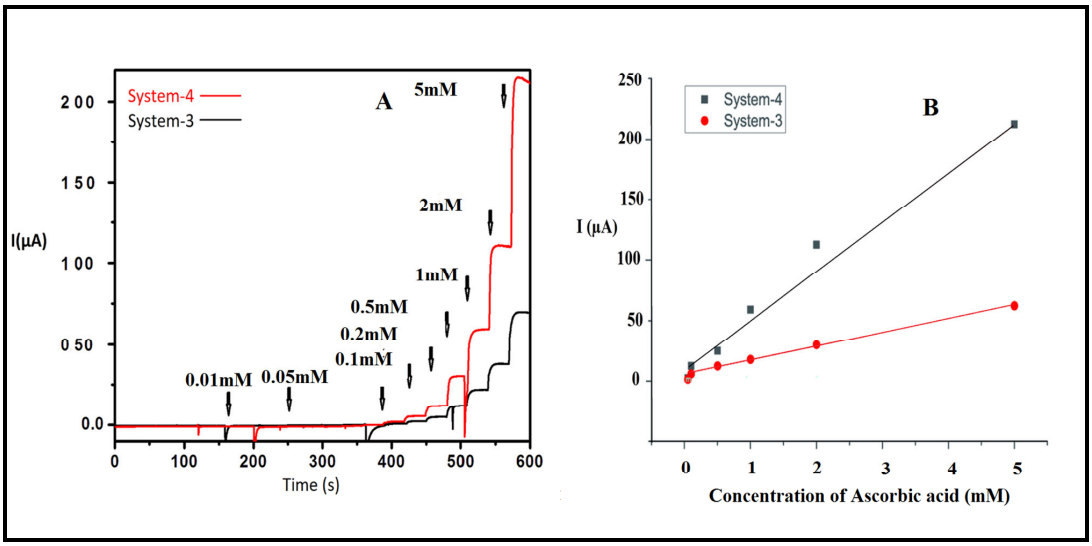

Fig. 7.8 (A) Time evolution of the current measured at constant voltage for system-3 (PANI/CMC) and system-4 (PANI/MWCNTs/CMC) in response to ascorbic acid subsequent injections in steps in PBS buffer of pH 7

7.3.8.3 Electrochemical Impedance Spectroscopy:

The EIS gives the information about charge transfer resistance of the solid-liquid interface due to additives and ascorbic acid using PBS-7 as an electrolyte *(c.f. C5D)*. Nyquist plots include two different regions: a semicircle in the high frequency and straight line in the low-frequency region. The semicircle in the high-frequency region stands for charge transfer resistance, double-layer capacitance and the straight line indicates that the reaction is controlled by interface diffusion between the electrolyte and electrode. The surface resistances greatly depend on the morphology and composition of the material. PANI/CMC and PANI/MWCNTs/CMC have higher impedance than PANI and PANI/MWCNTs, attributed to non-conductive nature of CMC. MWCNT decrease the resistance of system-2 and system-4. When the Ascorbic acid was introduced, the impedance atlas diameter of the sensor decreased indicating a greater number of charge transfers with higher mobility of the

charge carriers. This lower charge transfer resistance is due to the alignment of polymer chains.

7.3.8.4 Ink and Membrane Formation Ability:

CMC based conducting ink formulation has been developed by many research groups for printed electronics as an eco-friendly option (Magdassi et al. 2003; Karagiannidis et al. 2017; Barras et al. 2017). PANI/MWCNT/CMC composite material can be employed as conductive electroactive pigments. Nanocomposite material, graphite powder, and CMC solution were sonicated for about 15 minutes and a uniform and stable dispersion was obtained. The suspension was poured into a dish and kept for 5-6 hours, a membrane was obtained. This suspension could be used as electroactive ink and membrane applications *(c.f. C6A, B)*.

7.4 Conclusions:

We have successfully prepared an integrated green-nanocomposite material using PANI, MWCNTs and CMC. The ternary system is more complex than the binary system, attributed to multifold interaction among components. The developed material has a balance among the hydrophobic and hydrophilic characters, i.e. hydroxyl groups and bonded water molecules of CMC contributed to hydrophilic character, whereas a small amount of MWCNTs contributed to hydrophobic character. Nanotubes lead to a large surface area, higher stability (confirmed by TGA studies), and better electrochemical properties (confirmed from EIS, CV and amperometry). Morphological and BET studies confirmed that system-4 has integrated compact

granular structures (size ~50 nm, pore volume ~0.06 cm^3/g, pore size ~14 Å, average surface area is ~169m^2/g). The developed sensor showed good linear range from 0.05 mM to 5mM, sensitivity 100.63 $\mu AmM^{-1}cm^{-2}$ with a detection limit of 0.01 mM. The developed material is easily dispersed in the CMC hydrogel/solution. Good dispersion indicates that this material is a potential candidate for electroactive ink and membrane formation.